

Oscillation of the spin-currents of cold atoms on a ring due to light-induced spin-orbit coupling

Xie Wen-Fang ()

School of Physics and Electronic Engineering, Guangzhou University, Guangzhou 510006, People's Republic of China

He Yan-Zhang () and Bao Cheng-Guang (*)

School of Physics and Engineering, Sun Yat-Sen University, Guangzhou 510275, People's Republic of China.

(Dated: May 12, 2015)

The evolution of two-component cold atoms on a ring with spin-orbit coupling has been studied analytically for the case with N noninteracting particles. Then, the effect of interaction is evaluated numerically via a two-body system. Two cases are considered: (i) Starting from a ground state the evolution is induced by a sudden change of the laser field, and (ii) Starting from a superposition state. Oscillating persistent spin-currents have been found. A set of formulae have been derived to describe the period and amplitude of the oscillation. Based on these formulae the oscillation can be well controlled via adjusting the parameters of the laser beams. In particular, it is predicted that movable stripes might emerge on the ring.

PACS numbers: 03.75.Kk, 03.75.Mn, 03.75.Nt

Keywords: light-induced spin-orbit coupling, spin-currents of cold atoms, condensates on a ring

I. INTRODUCTION

It is well known that the study of the motion of charged particles under a magnetic field is an essential topic in both macroscopic and microscopic physics. In particular, a number of distinguished quantum mechanic phenomena, such as the Aharonov-Bohm (A-B) oscillation and the fractional quantum Hall effect (FQHE), are caused by the magnetic gauge field.[1–3] After the experimental realization of the condensation of neutral atoms with nonzero spin,[4] a great interest is to create a light-induced gauge vector field to achieve the spin-orbit coupling (SOC) so that various magnetic-electronic phenomena of charged particles occurring in condense matters can be copied into the world of condensates of neutral atoms.[5–9] Since 2005 there are proposals by the theorists for producing the light-induced gauge vector field for the condensates with multi-component neutral cold atoms.[10–15] The first experimental realization of the SOC in condensates was implemented in 2009 by dressing the cold atoms with two counter propagating polarized laser beams.[16, 17] This technique opens a new perspective in the field of BEC, more and more experimental[18–21] and theoretical [22–24] results are reported. It was found that the total magnetization (or spin-polarizability, which measures the difference of the densities of the spin-components) varies with time. It implies the existence of spin-currents.[12, 16, 22] Besides, the collective-mode dynamics has been studied, the spatial motions along different directions could be correlated (say, a dipole mode might induce a breathing mode in its perpendicular plane).[24] The instability caused by the collective mode has also been studied.[23]

On the other hand it is now possible to trap a condensate in ring geometry. Long-lived rotational superflows have been induced in this kind of systems.[20, 25–33] The creation of the spin-currents of two-component condensates on a ring, due to the introduction of the laser beams, has been experimentally realized.[20] It was found that the stability depends strongly on the initial ratio of the two components.[20] However, the oscillation of the spin-currents on the ring has not yet been observed.

Obviously, the study of the cold spin-currents (i.e., the current of each spin-component) caused by the SOC is just beginning. It is expected that the oscillation of the spin-currents might also emerge in the ring geometry (because a circular motion is equivalent to a linear motion with a periodic boundary condition). To confirm this suggestion, a one-dimensional model of the two-component condensates on a ring under SOC is adopted in this paper. The aim is to clarify from the theoretical aspect how the details of oscillation (the period and amplitude) depend on the parameters of the laser beams. We believe that the interaction might not be crucial. Therefore, the interaction is neglected firstly so as to emphasize the decisive role of the laser beams. Then, the effect of the interaction is evaluated via a two-body system.

II. TIME-DEPENDENT SOLUTION

Let the quasi-spin \hat{s} be introduced to describe the two components of an atom as usual. The atomic state with $s_z = 1/2$ ($-1/2$) is named the up- (down-) state. When two counter-propagating and polarized laser beams are applied, due to the SOC, the two components of atoms might move towards opposite directions along the beams and can transform to each other via a spin-flip. When the interaction is neglected, the Hamiltonian is just $H =$

*Corresponding author: stsbcg@mail.sysu.edu.cn

$\Sigma_i \hat{h}_i$, where \hat{h}_i is for the i -th particle. Neglecting the subscript i ,

$$\hat{h} = \begin{pmatrix} -\frac{\partial^2}{\partial \theta^2} + \delta, & \gamma e^{-2i\beta\theta} \\ \gamma e^{2i\beta\theta}, & -\frac{\partial^2}{\partial \theta^2} - \delta \end{pmatrix}, \quad (1)$$

where θ is the azimuthal angle along the ring.[9] The unit of energy is hereafter $E_{\text{unit}} \equiv \hbar^2/(2mR^2)$, where m is the mass of an atom, R is the radius of the ring. $\beta \equiv k_0 R$, where $2k_0$ is the momentum transfer caused by the two lasers. $\gamma \equiv \frac{\Omega}{2E_{\text{unit}}}$, where $\Omega/2$ is the strength of Raman coupling causing the spin-flips accompanied by the momentum transfer. Let $\varepsilon_{\text{split}}$ be the Zeeman energy difference between the two spin-states, and ω_δ is the frequency difference between the two laser beams. We define the Raman detuning $\delta \equiv (\varepsilon_{\text{split}} - \hbar\omega_\delta)/(2E_{\text{unit}})$. In addition to γ , δ is an important quantity because it can be tuned so that the related process could be energy-adapted (see below). Note that, due to the ring geometry, 2β must be an integer. It implies that the transfer of momentum will be suppressed unless the transfer is close to a specific set of values depending on R . Thus, an additional constraint is required under the ring geometry.

To illustrate the connection with conventional SO coupling, we define a U -transformation so that the up-state (down-state) is multiplied by a factor $e^{i\beta\theta}$ ($e^{-i\beta\theta}$). Then, by introducing the Pauli matrices σ_z and σ_x , $U\hat{h}U^{-1}$ can be written in a more familiar form as [9, 12, 16, 34, 35]

$$U\hat{h}U^{-1} = (-i\sigma_I \frac{\partial}{\partial \theta} - \beta\sigma_z)^2 + \delta\sigma_z + \gamma\sigma_x, \quad (2)$$

where σ_I is just a unit matrix with rank 2.

\hat{h} has two groups of eigenstates, they can be written as [16, 34, 35]

$$\psi_k^{(+)} = \sin(\rho_k)\varphi_{k-\beta,\uparrow} + \cos(\rho_k)\varphi_{k+\beta,\downarrow}, \quad (3)$$

$$\psi_k^{(-)} = \cos(\rho_k)\varphi_{k-\beta,\uparrow} - \sin(\rho_k)\varphi_{k+\beta,\downarrow}, \quad (4)$$

where

$$\varphi_{k\pm\beta,\uparrow} = \frac{1}{\sqrt{2\pi}} e^{i(k\pm\beta)\theta} \begin{pmatrix} 1 \\ 0 \end{pmatrix}, \quad (5)$$

$$\varphi_{k\pm\beta,\downarrow} = \frac{1}{\sqrt{2\pi}} e^{i(k\pm\beta)\theta} \begin{pmatrix} 0 \\ 1 \end{pmatrix}. \quad (6)$$

k is an integer (half-integer) when β is an integer (half-integer), $\sin \rho_k = s_\gamma \sqrt{(a_k - 2k\beta + \delta)/(2a_k)}$, $\cos \rho_k = \sqrt{(a_k + 2k\beta - \delta)/(2a_k)}$, s_γ is the sign of γ , $a_k = \sqrt{(2k\beta - \delta)^2 + \gamma^2}$, and ρ_k is ranged from $-\pi/2 \rightarrow \pi/2$. One can see that the eigenstates have two notable features:

(i) Each of them contains both the up and down components, they are propagating with angular momenta $k - \beta$ and $k + \beta$, respectively. Where 2β is proportional to the momentum transfer caused by the counter-propagating laser beams.

(ii) In each $\psi_k^{(\pm)}$ the weights of the two components can be controlled by tuning δ . When $\delta < 2k\beta$, we have $-\pi/4 \leq \rho_k \leq \pi/4$, and therefore the weight of the up-component is larger in $\psi_k^{(-)}$ but smaller in $\psi_k^{(+)}$. Whereas when $\delta > 2k\beta$, $\psi_k^{(-)}$ will contain more down-component. In particular, when δ is tuned so that $\delta = 2k\beta$, the weights of the two components in all the eigenstates are equal.

The eigenenergies of $\psi_k^{(\pm)}$ are $E_k^{(\pm)} = k^2 + \beta^2 \pm a_k$. Obviously, $E_k^{(-)} \leq E_k^{(+)}$.

The time-dependent solution $\psi(\theta, t)$ of the single-particle Schrödinger equation starting from an initial state ψ_{init} can be formally written as

$$\begin{aligned} \psi(\theta, t) &= e^{-i\tau\hat{h}}\psi_{\text{init}} \\ &= \sum_{k\lambda} |\psi_k^{(\lambda)}\rangle e^{-i\tau E_k^{(\lambda)}} \langle \psi_k^{(\lambda)} | \psi_{\text{init}} \rangle, \end{aligned} \quad (7)$$

where $\tau \equiv tE_{\text{unit}}/\hbar$ (for ^{87}Rb and $R = 12\mu\text{m}$ as given in [20], $t = 0.398\tau\text{sec}$), $\lambda = \pm$, k runs over the (half-) integers when β is an (half-) integer.

III. EVOLUTION CAUSED BY A SUDDEN CHANGE OF THE LASER FIELD

In the experiment reported in [21] a strong oscillation of the magnetization induced by a sudden change of the laser field was reported. It is assumed that a set of parameters β , γ_1 , and δ_1 (the first set) are given initially, and the initial state is just the ground state (g.s.) of \hat{h} as $\psi_{\text{init}} = \psi_{\text{gs}} = \cos(\rho_q^{(1)})\varphi_{q-\beta,\uparrow} - \sin(\rho_q^{(1)})\varphi_{q+\beta,\downarrow}$, where q depends on the three parameters so that the associated energy $E_q^{(-)}$ is the lowest. The superscript in $\rho_q^{(1)}$ implies that it is obtained from the first set of parameters. Then, γ_1 and δ_1 are suddenly changed to γ_2 and δ_2 (the second set). Accordingly, we have a new Hamiltonian and a new set of eigenstates. With them $\psi(\theta, t)$ becomes

$$\psi(\theta, t) = e^{-i\tau(q^2 + \beta^2)} (f_u \varphi_{q-\beta,\uparrow} - f_d \varphi_{q+\beta,\downarrow}), \quad (8)$$

where $f_u = \cos(\rho_q^{(1)})\cos(a_q^{(2)}\tau) + i\cos(2\rho_q^{(2)} - \rho_q^{(1)})\sin(a_q^{(2)}\tau)$, and $f_d = \sin(\rho_q^{(1)})\cos(a_q^{(2)}\tau) + i\sin(2\rho_q^{(2)} - \rho_q^{(1)})\sin(a_q^{(2)}\tau)$. Where $a_q^{(2)}$ and $\rho_q^{(2)}$ are obtained from γ_2 and δ_2 . From $\psi(\theta, t)$, we know that the two components of the g.s., $\varphi_{q-\beta,\uparrow}$ and $\varphi_{q+\beta,\downarrow}$, remain unchanged. However, the coefficients of composition are no more constants but oscillate with τ .

Let the time-dependent densities of the up- and down-component be defined from the identity $\psi^+(\theta, t)\psi(\theta, t) \equiv$

$n_\uparrow(\theta, \tau) + n_\downarrow(\theta, \tau)$. Then, we have

$$n_\uparrow = \frac{1}{2\pi} \{ \cos^2(\rho_q^{(1)}) + [\cos^2(2\rho_q^{(2)} - \rho_q^{(1)}) - \cos^2(\rho_q^{(1)})] \times \sin^2(a_q^{(2)}\tau) \}, \quad (9)$$

$$n_\downarrow = \frac{1}{2\pi} \{ \sin^2(\rho_q^{(1)}) + [\sin^2(2\rho_q^{(2)} - \rho_q^{(1)}) - \sin^2(\rho_q^{(1)})] \times \sin^2(a_q^{(2)}\tau) \}. \quad (10)$$

The magnetization (or spin-polarization) is defined as $P_z = (n_\uparrow - n_\downarrow)/(n_\uparrow + n_\downarrow)$. We have

$$P_z = \cos(2\rho_q^{(1)}) + [\cos(4\rho_q^{(2)} - 2\rho_q^{(1)}) - \cos(2\rho_q^{(1)})] \times \sin^2(a_q^{(2)}\tau). \quad (11)$$

This formula gives a clear picture of a harmonic θ -independent oscillation with a period $\tau_p = \pi/a_q^{(2)}$ and an amplitude $A_{\text{amp}} = |\cos(4\rho_q^{(2)} - 2\rho_q^{(1)}) - \cos(2\rho_q^{(1)})|$.

Based on the second set of parameters let us define the energy difference of the two components as $E_{\text{diff}}^{(2)} \equiv \frac{1}{2} |\langle \varphi_{q-\beta, \uparrow} | \hat{h}^{(2)} | \varphi_{q-\beta, \uparrow} \rangle - \langle \varphi_{q+\beta, \downarrow} | \hat{h}^{(2)} | \varphi_{q+\beta, \downarrow} \rangle| = (2q\beta - \delta_2)$. Then, the frequency of oscillation $1/\tau_p =$

$\frac{1}{\pi} \sqrt{(E_{\text{diff}}^{(2)})^2 + \gamma_2^2}$. This formula demonstrates that both the strength of the Raman coupling and the energy difference are crucial. A larger $|\gamma_2|$ leads always to a higher frequency $\geq |\gamma_2|/\pi$. This frequency can be further tuned by varying δ_2 around $2q\beta$. In particular, when δ_2 is tuned so that $E_{\text{diff}}^{(2)}$ is zero, $1/\tau_p$ will arrive at its conditional minimum $|\gamma_2|/\pi$. Since $E_{\text{diff}}^{(2)}$ depends on q but not on the other details of the initial state, $1/\tau_p$ depends essentially on the second set of parameters when q is given.

On the other hand, the amplitude A_{amp} depends on both sets of parameters explicitly. When the first set of parameter has been given so that $\rho_q^{(1)}$ is fixed, A_{amp} will arrive at its conditional maximum at a specific value of $\rho_q^{(2)}$, namely, $\rho_q^{(2)} = \rho_q^{(1)}/2$ (if $\gamma_2 < 0$ and $\rho_q^{(1)} < -\pi/4$), or $= \rho_q^{(1)}/2 + \pi/2$ (if $\gamma_2 > 0$ and $\rho_q^{(1)} < -\pi/4$), or $= \rho_q^{(1)}/2 - \pi/4$ (if $\gamma_2 < 0$ and $-\pi/4 \leq \rho_q^{(1)} \leq \pi/4$), or $= \rho_q^{(1)}/2 + \pi/4$ (if $\gamma_2 > 0$ and $-\pi/4 \leq \rho_q^{(1)} \leq \pi/4$), or $= \rho_q^{(1)}/2 - \pi/2$ (if $\gamma_2 < 0$ and $\rho_q^{(1)} > \pi/4$), or $= \rho_q^{(1)}/2$ (if $\gamma_2 > 0$ and $\rho_q^{(1)} > \pi/4$). It implies that, no matter how the first set of parameters are, one can tune the second set so that the amplitude is conditionally maximized, namely, $A_{\text{amp}} = 1 + |\cos(2\rho_q^{(1)})|$. In particular, when $\gamma_1 = 0$, we have $\rho_q^{(1)} = \pm\pi/2$ or 0. In this case, if $\gamma_2 \neq 0$ and δ_2 is tuned so that $E_{\text{diff}}^{(2)} = 0$, then $\rho_q^{(2)} = (\gamma_2/|\gamma_2|)\pi/4$ and the amplitude would arrive at its absolute maximum, namely, $A_{\text{amp}} = 2$. Note that the condition $\rho_q^{(1)} = \pm\pi/2$ or 0 implies that the initial state is pure without mixing (namely, either $\psi_{\text{init}} = \varphi_{q-\beta, \uparrow}$ or $\varphi_{q+\beta, \downarrow}$), while the fact $A_{\text{amp}} = 2$ implies a complete transformation of the two components (namely, from a pure up-state to a pure down-state, or vice versa). Therefore, $\gamma_1 = 0$ is required so that the maximal amplitude could be realized. On the

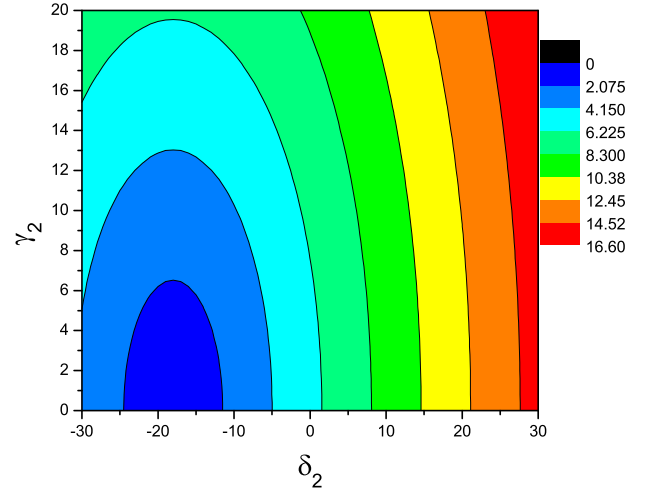


FIG. 1: The frequency $1/\tau_p$ versus δ_2 and γ_2 . The oscillation is caused by a sudden change in γ and δ . $\beta = 3$ and $q = -3$ are given. The values of the contours are in an arithmetic series. The contour closest to the right side has the largest value $1/\tau_p = 14.5$.

other hand, in any cases, when γ_2 and γ_1 have the same sign and $\rho_q^{(2)} \rightarrow \rho_q^{(1)}$, or γ_2 and γ_1 have opposite signs and $\rho_q^{(2)} \rightarrow \rho_q^{(1)} \pm \pi/2$, $A_{\text{amp}} \rightarrow 0$ and the oscillation damps. This is obvious from the expression of A_{amp} .

In addition to the densities, one can further define the current based on the equation of continuity as $-\frac{\partial}{\partial t}(\psi^\dagger(\theta, t)\psi(\theta, t)) = \frac{\partial j}{\partial \theta}$. From this definition we found that the current $j = j_\uparrow + j_\downarrow$ in which $j_\uparrow \equiv j_{\text{unit}} n_\uparrow(q - \beta)$ is the current of the up-component and is named up-current, while $j_\downarrow \equiv j_{\text{unit}} n_\downarrow(q + \beta)$ is the down-current, where the unit is $j_{\text{unit}} = \hbar/(mR^2)$. [23] The currents are also oscillating with the same period $\pi/a_q^{(2)}$, and they are also θ -independent. Obviously, when $|\beta| > |q|$, j_\uparrow and j_\downarrow will have different signs. Therefore, counter propagating currents emerge. This is a distinguished feature.

The above formulae arise from a single-particle Hamiltonian. For N-particle systems, when all the particles fall into the same state ψ_{gs} initially and the interaction is neglected, it is straight forward to prove that the above formulae hold also.

To give numerical results, the radius is given at $R = 12\mu\text{m}$ in this paper. A contour diagram for the frequency $1/\tau_p$ versus γ_2 and δ_2 is shown in Fig.1. Where the minimum is located at $\gamma_2 = 0$ and $E_{\text{diff}}^{(2)} = 0$ (namely, $\delta_2 = 2q\beta = -18$), at which the oscillation vanishes.

Two contour diagrams for A_{amp} versus γ_2 and δ_2 with γ_1 and δ_1 being fixed are shown in Fig.2, where all the contours appear as straight lines. This arises from the fact that $\rho_q^{(2)}$ can be rewritten as a function of $|\gamma_2/E_{\text{diff}}^{(2)}| = |\gamma_2/(\delta_2 - 2q\beta)|$ together with the two signs of γ_2 and $\delta_2 - 2q\beta$ (it implies that a given $\rho_q^{(2)}$ is associ-

ated with a straight line on the $\delta_2 - \gamma_2$ plane). In Fig. 2a (b) the given values of β , γ_1 , and δ_1 lead to $q = -3$ (3) and $\rho_q^{(1)} = 0.435\pi$ (0.0653π). According to the discussion given previously and when $\gamma_2 > 0$, the maximum of A_{amp} should appear when $\rho_q^{(2)} = \rho_q^{(1)}/2 = 0.218\pi$ in Fig. 2a, and $\rho_q^{(2)} = \rho_q^{(1)}/2 + \pi/4 = 0.315\pi$ in 2b. This maximum is associated with the straight dotted line marked in the figure (Incidentally, if $\rho_q^{(2)} = \pi/4$, then the associated straight line would be vertical. Since the two dotted lines have their $\rho_q^{(2)}$ close to $\pi/4$, they are nearly vertical). Whereas when $\rho_q^{(2)} = \rho_q^{(1)}$, the associated straight line is marked by a solid line in the figure (where the small circle marks the place that $\gamma_2 = \gamma_1$, and $\delta_2 = \delta_1$). Three notable features are reminded:

(i) The frequency does not depend on the first set of parameters, except q . A larger $|\gamma_2|$ leads always to a higher frequency which can be further tuned by varying δ_2 around $2q\beta$. When $\delta_2 = 2q\beta$, the frequency arrives at its conditional minimum $|\gamma_2|/\pi$.

(ii) A_{amp} depends on the ratios γ_1/δ_1 and γ_2/δ_2 . When γ_2 and δ_2 are given along the solid line (the slope of this line depends on γ_1/δ_1), the sudden change of $\gamma_1 \rightarrow \gamma_2$ and $\delta_1 \rightarrow \delta_2$ can not cause an evolution (i.e., $A_{\text{amp}} = 0$). When γ_2 and δ_2 are given along the dotted line (also depends on γ_1/δ_1), the amplitude will remain unchanged and is conditionally maximized, namely, $A_{\text{amp}} = 1 + |\cos(2\rho_q^{(1)})|$. In any cases, *one can always tune δ_2 so that the amplitude is either suppressed or conditionally maximized.*

(iii) Due to the fact that the contours are straight lines, when γ_2 is small ($\neq 0$) there is a narrow domain of δ_2 surrounding $2q\beta$ in which A_{amp} is highly sensitive to δ_2 and appears as a sharp peak. At the peak the amplitude is large while the associated frequency is low.

IV. EVOLUTION INITIATED FROM A SUPERPOSITION STATE

Recently, the initial state was prepared in a superposition state in an experiment of cold atoms with the ring geometry.[20] In this experiment an additional radio frequency field was used for preparing the initial state

$$\psi_{\text{init}} = \sin(\phi/2)\varphi_{q\uparrow} + \cos(\phi/2)\varphi_{q\downarrow}, \quad (12)$$

where ϕ determines the initial ratio of the two components and is tunable ($0 \leq \phi \leq \pi$). q is a tunable integer and marks the initial angular momentum of the particle. In this case we have the set of parameters ϕ , q , β , γ , and δ . The corresponding time-dependent solution is

$$\begin{aligned} \psi(\theta, t) = e^{-i\tau(q^2+2\beta^2)} & (f_{u_1}\varphi_{q,\uparrow} + f_{u_2}\varphi_{q-2\beta,\uparrow} \\ & + f_{d_1}\varphi_{q+2\beta,\downarrow} + f_{d_2}\varphi_{q,\downarrow}), \end{aligned} \quad (13)$$

where $f_{u_1} = \sin(\phi/2)e^{-2iq\beta\tau}[\cos(a_{q+\beta}\tau) + i\cos(2\rho_{q+\beta})\sin(a_{q+\beta}\tau)]$, $f_{u_2} =$

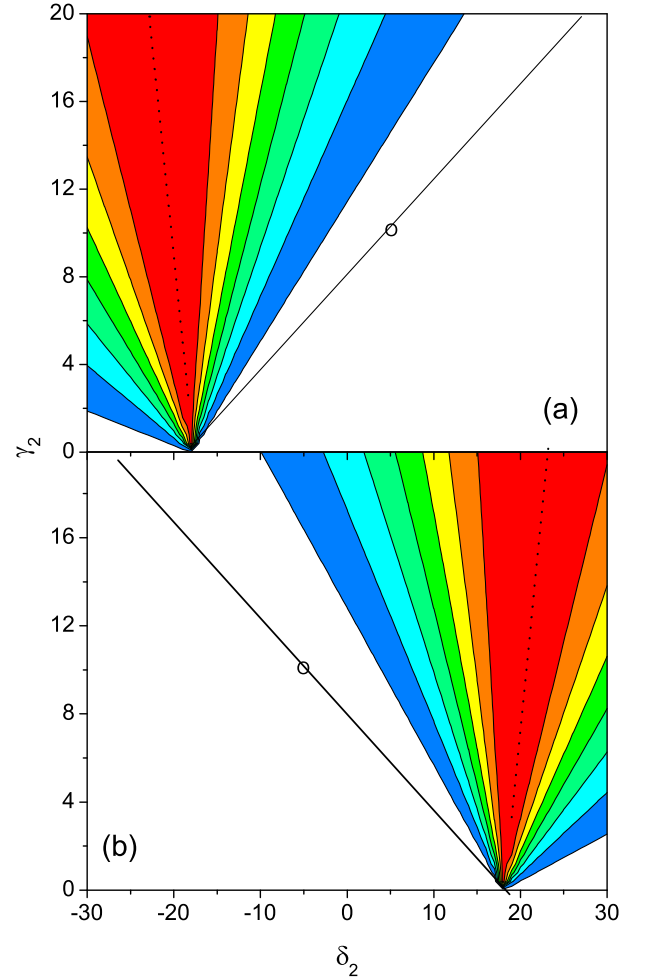


FIG. 2: The amplitude A_{amp} versus δ_2 and γ_2 . $\beta = 3$, $\gamma_1 = 10$, and $\delta_1 = 5(-5)$, are given in a (b). Accordingly, $q = -3$ (3) in a (b). The oscillation is caused by a sudden change from γ_1 to γ_2 and δ_1 to δ_2 . The dotted line marks the locations where $\rho_q^{(2)} = \rho_q^{(1)}/2$ (a), or $\rho_q^{(2)} = \rho_q^{(1)}/2 + \pi/4$ (b). Thus this line marks the conditional maximum of $A_{\text{amp}} = 1 + |\cos(2\rho_q^{(1)})| = 1.917$ in both (a) and (b), which is the largest value in each panel. The contours going away from this line are in an arithmetic series and decrease to zero. The black small circle marks the location where $\delta_2 = \delta_1$ and $\gamma_2 = \gamma_1$. The solid line passing through the circle marks the locations where $\rho_q^{(2)} = \rho_q^{(1)}$ and accordingly $A_{\text{amp}} = 0$.

$$\begin{aligned} -i\cos(\phi/2)e^{2iq\beta\tau}\sin(2\rho_{q-\beta})\sin(a_{q-\beta}\tau) & , \quad f_{d_1} = \\ -i\sin(\phi/2)e^{-2iq\beta\tau}\sin(2\rho_{q+\beta})\sin(a_{q+\beta}\tau), & \text{ and } f_{d_2} = \\ \cos(\phi/2)e^{2iq\beta\tau}[\cos(a_{q-\beta}\tau) - i\cos(2\rho_{q-\beta})\sin(a_{q-\beta}\tau)]. & \end{aligned}$$

Accordingly, we can obtain the up- and down-densities $n_{\uparrow}(\theta, \tau)$ and $n_{\downarrow}(\theta, \tau)$ given in the appendix. From them the magnetization P_z can be obtained. It is apparent that, when $\phi = \pi$ or 0 (i.e., ψ_{init} is a pure up-state or down-state) the magnetization has a very simple form as

$$P_z = \cos(4\rho_{q+\beta}) + (1 - \cos(4\rho_{q+\beta}))\cos^2(a_{q+\beta}\tau), \quad (14)$$

if $\phi = \pi$, or

$$P_z = -\cos(4\rho_{q-\beta}) - (1 - \cos(4\rho_{q-\beta}))\cos^2(a_{q-\beta}\tau), \quad (15)$$

if $\phi = 0$.

These formulae also give a clear picture of harmonic oscillation, but the periods are different for the two cases of ϕ .

When $\phi = \pi$, $\tau_p = \pi/a_{q+\beta}$. If δ is tuned so that $\delta = 2(q+\beta)\beta \equiv \delta_o$, the frequency will be minimized, namely, $(1/\tau_p)_{\min} = \frac{1}{\pi}|\gamma|$. When δ goes away from δ_o , the frequency increases. The amplitude $A_{\text{amp}} = 1 - \cos(4\rho_{q+\beta})$. Obviously, when $\delta = \delta_o$, we have $\rho_{q+\beta} = \pm\pi/4$, and the amplitude would arrive at its maximum, namely, $(A_{\text{amp}})_{\max} = 2$. Further more, when $\gamma \rightarrow \pm 0$, one can prove that $\rho_{q+\beta}$ will tend to 0 or $\pm\pi/2$. In any of these cases $A_{\text{amp}} = 0$ and the oscillation disappear. This implies that γ is the source of the oscillation.

When $\phi = 0$, the discussion in the preceding paragraph holds also, except that $q + \beta$ should be changed to $q - \beta$, and δ_o should be replaced by $2(q - \beta)\beta$. An example of A_{amp} is shown in Fig.3. Fig.3 is of a similar form to Fig.2 (all the contours are straight lines converge to a point with $\gamma = 0$) except that the dotted line in the former is exactly vertical.

When ϕ is neither π nor 0, the oscillation is no more harmonic. In particular, both the up- and down-densities depend on θ (refer to the appendix). It implies that the densities are not uniform on the ring as before. Consequently, stripes emerge along the ring, and the stripes move with time. An example of the evolution of P_z is shown in Fig.4. Where the relation $\delta = 2(q + \beta)\beta$ holds. Accordingly, the curve with $\phi = \pi$ has the maximized $A_{\text{amp}} = 2$ and a minimized frequency. Whereas the curve with $\phi = 0$ has a smaller A_{amp} and a larger frequency. For $\phi = \pi/2$, the anharmonic oscillation is clearly shown.

An example of the up-density versus θ with $\phi = \pi/2$ is shown in Fig.5, where the stripes emerge along the ring. Note that two waves $\varphi_{q,\uparrow}$ and $\varphi_{q-2\beta,\uparrow}$ are contained in the up-component, and $\varphi_{q,\downarrow}$ and $\varphi_{q+2\beta,\downarrow}$ in the down-component. The stripes arise from the interference of these waves. Note that one of these waves contains an additional factor $e^{\mp i2\beta\theta}$. Accordingly, the stripes appear periodically with θ as shown in Fig.5 and the number of peaks (valleys) in the domain $(0, 2\pi)$ is 2β (say, the number is four in Fig.5, where $\beta = 2$). The locations of the peaks of the stripes move with time, the magnitudes of the peaks also change with time.

As before, when all the particles are given in the same ψ_{init} initially and the interaction is neglected, the above formulae and discussion hold also for N-particle systems.

V. EVALUATION OF THE EFFECT OF INTERACTION

When the interaction is taken into account, the total Hamiltonian is $H = \sum_i \hat{h}_i + \sum_{i<j} V_{ij}$, where $V_{ij} = g\delta(\theta_i - \theta_j)$, $g = g_{\uparrow\uparrow}$ (if both atoms are up), $g_{\downarrow\downarrow}$ (both

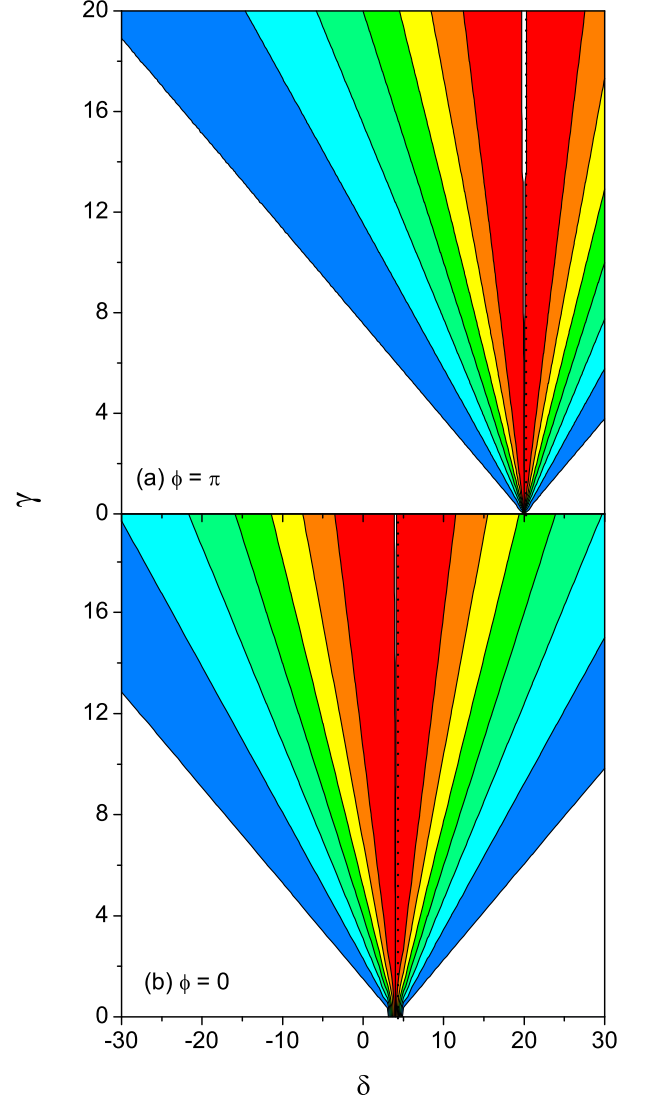


FIG. 3: The amplitude A_{amp} versus δ and γ for the case that the initial state is a superposition state. $q = 3$ and $\beta = 2$ are assumed. $\phi = \pi(0)$ are given in (a) (b). The dotted line marks the maximum of $A_{\text{amp}} = 2$. The locations with $\gamma = 0$ have $A_{\text{amp}} = 0$.

down), or $g_{\uparrow\downarrow}$ (one up and one down). In order to evaluate the effect of interaction in the simplest way, we study a two-body system. Firstly, a set of single particle states $\varphi_{k\mu} = \frac{1}{\sqrt{2\pi}}e^{ik\theta}\chi_\mu$, where $\chi_\mu = \begin{pmatrix} 1 \\ 0 \end{pmatrix}$ or $\begin{pmatrix} 0 \\ 1 \end{pmatrix}$, and $-k_{\max} \leq k \leq k_{\max}$, are adopted. Accordingly, we have $2(2k_{\max} + 1)$ single particle states, and they are renamed as $\varphi_j \equiv \varphi_{k_j\mu_j}$. Based on φ_j a set of basis functions for the two-body system $\Phi_i = \tilde{S}[\varphi_j(1)\varphi_{j'}(2)]$ are defined, where \tilde{S} is for the symmetrization and normalization, and $j \geq j'$.

Note that the strength of a pair of realistic Rb atoms is $g_{\text{Rb}} = 7.79 \times 10^{-12} \text{Hz cm}^3$ (the differences in the strengths between the up-up, up-down, and down-down

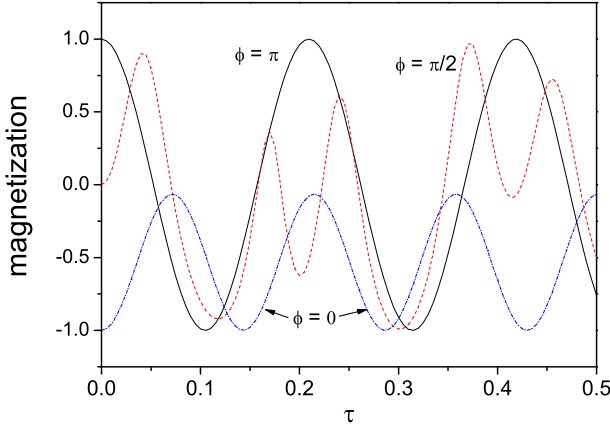


FIG. 4: The magnetization P_z versus τ observed at $\theta = 0$ for the case that the initial state is a superposition state with a ϕ marked by the curve. $q = 3$, $\beta = 2$, $\gamma = 15$, and $\delta = 20$ are assumed. When $\phi = \pi$ or 0 the oscillation is harmonic. Otherwise, it is not.

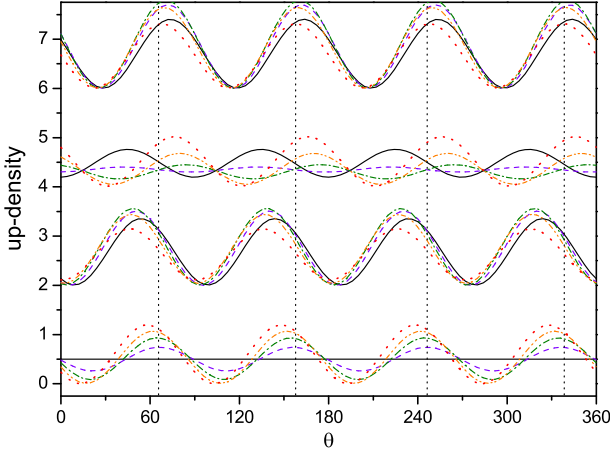


FIG. 5: Up-density n_{\uparrow} versus θ with $\phi = \pi/2$. The densities are given by 20 curves for a sequence of τ . Starting from $\tau = 0$, in each step τ is increased by $1/40$. The 20 curves in the sequence are divided into 4 groups. The n_{\uparrow} of each group has been shifted up by 2 relative to its preceding group, for a clearer perspective. The five n_{\uparrow} in each group are plotted in solid, dash, dash-dot, dash-dot-dot, and dot lines, respectively, according to the time-sequence ($\tau = 0$ is the horizontal solid line in the lowest group). The parameters are $q = 1$, $\beta = 2$, $\gamma = 10$, and $\delta = 1$. The vertical dotted lines are also for guiding the eyes.

pairs are very small and are therefore neglected). Since the atoms in related experiments are not distributed exactly on a one-dimensional ring but in a domain surrounding the ring, the effect of the diffused distribution should be considered. Hence, for each $\varphi_{k\mu}$ we define its 3-dimensional counterpart $\varphi_{k\mu}^{[3d]} = \frac{1}{\pi r_w} \sqrt{\frac{1}{R}} e^{ik\theta} e^{-(r/r_w)^2} \chi_{\mu}$, where the Gaussian function $e^{-(r/r_w)^2}$ describes the dif-

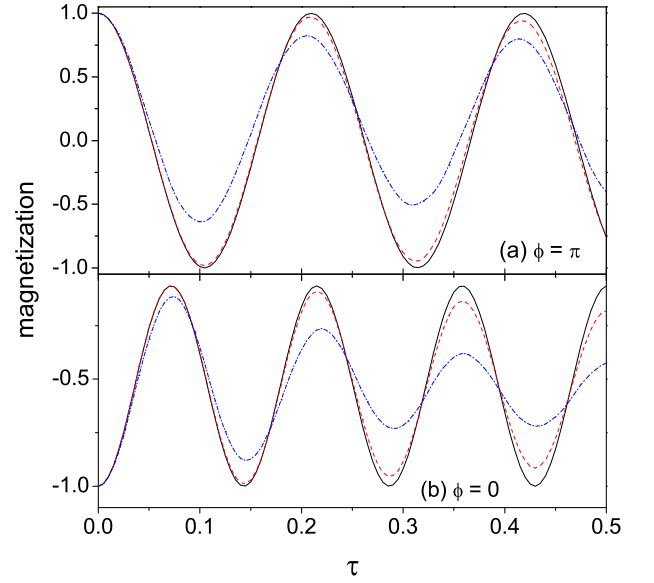


FIG. 6: P_z of a 2-body system of Rb atoms versus τ with interaction $V_{ij} = g\delta(\theta_i - \theta_j)$, $g = 0$ (solid), $100g_{\text{eff}}$ (dash), and $2000g_{\text{eff}}$ (dash-dot). The initial state has $\phi = \pi$ (a) and $= 0$ (b). $r_w = R/\sqrt{18}$. The other parameters are the same as in Fig.4

fused distribution and r_w measures the width of the distribution. With $\varphi_{k\mu}^{[3d]}$ we define an effective strength g_{eff} so that for any pair of matrix elements

$$g_{\text{eff}} \int d\theta_i d\theta_j \varphi_{k_1\mu_1}^\dagger \varphi_{k_2\mu_2}^\dagger \delta(\theta_i - \theta_j) \varphi_{k_3\mu_3} \varphi_{k_4\mu_4} \\ = g_{\text{Rb}} \int d\mathbf{r}_i d\mathbf{r}_j \varphi_{k_1\mu_1}^{[3d]\dagger} \varphi_{k_2\mu_2}^{[3d]\dagger} \delta(\mathbf{r}_i - \mathbf{r}_j) \varphi_{k_3\mu_3}^{[3d]} \varphi_{k_4\mu_4}^{[3d]}. \quad (16)$$

Then, we have $g_{\text{eff}} = \frac{1}{\pi R r_w^2} g_{\text{Rb}}$ which is the effective strength adopted in our calculation.

It is assumed that both atoms are given at the same superposition state with $\phi = \pi$ or 0 initially. When the Hamiltonian is diagonalized in the space expanded by Φ_i , the eigenenergies E_l and eigenstates $\Psi_l \equiv \sum_i C_{li} \Phi_i$ can be obtained, and the time-dependent state is

$$\Psi(\theta, t) = \sum_l e^{-i\tau E_l} \Psi_l \langle \Psi_l | \Psi_{\text{init}} \rangle, \quad (17)$$

where $\Psi_{\text{init}} = \psi_{\text{init}}(1)\psi_{\text{init}}(2)$. From $\Psi(\theta, t)$ the densities and $P_z(t)$ can be calculated. An examples with $k_{\text{max}} = 14$ is shown in Fig.6 where the strength g is given at three values. When k_{max} is changed from 14 to 12, there is no explicit changes in the pattern. It implies that the choice $k_{\text{max}} = 14$ is sufficient in qualitative sense.

In Fig.6 the curves "1" and "2" overlap approximately. It implies that the effect of interaction with a $g \leq 100g_{\text{eff}}$ is very small. However, when $g = 2000g_{\text{eff}}$, the amplitude decreases with time explicitly as shown by the dash-dot curve, while the period remains nearly unchanged. Note

that, based on the Gross-Pitaevskii equation, the effect of the combined interaction imposing on a single particle from the other $N - 1$ particles is similar to an appropriate strengthening of the strength of the atom-atom interaction. Thus the explicit damp that happens when $g = 2000g_{\text{eff}}$ implies that, for an N -body system with a larger N , the damp would actually occur. This is a topic to be clarified further. In fact, the damp of the oscillation has already been observed in all related existing experiments.[16, 21]

VI. SUMMARY

In summary, the oscillation of the cold atoms under the SOC and constrained on a ring has been studied analytically without taking the interaction into account. Then, the effect of the interaction is evaluated numerically via a two-body system. Two cases, namely, the evolution that starts from a g.s. and is induced by a sudden change of the laser field, and the evolution that starts from a superposition state, are involved. The emphasis is placed on clarifying the relation between the parameters of the laser beams and the period and amplitude of the oscillation. This is achieved by giving a set of formulae so that the relation can be understood analytically. The con-

ditions that the frequency and/or the amplitude can be maximized or minimized have been predicted. To realize the mutual-transformation of the two components, not only the strength of the Raman coupling γ is important, the energy difference between the two components is also important which can be tuned by δ (this is similar to the case of a resonance). The frequency of oscillation will increase with γ in general, while the amplitude depends on the interrelation of γ and δ . When (δ, γ) vary along a specific straight line on the $\delta - \gamma$ plane, the amplitude may increase, decrease, or even remain unchanged depending on the slope of the line. This is a common feature for the first case and for the second case with $\phi = \pi$ or 0 . Whereas when $\phi \neq \pi$ and 0 , movable stripes will emerge on the ring. Experimental confirmation of the regularity unveiled in this paper and the predicted phenomena is expected.

The support from the NSFC (China) under the grant number 10874249 is appreciated.

Appendix

When the initial state is $\psi_{\text{init}} = \sin(\phi/2)\varphi_{q\uparrow} + \cos(\phi/2)\varphi_{q\downarrow}$, the associated up- and down-densities during the evolution are

$$\begin{aligned} n_{\uparrow}(\theta, \tau) = & \frac{1}{2\pi} \{ \sin^2(\phi/2) [\cos^2(a_{q+\beta}\tau) + \cos^2(2\rho_{q+\beta}) \sin^2(a_{q+\beta}\tau)] \\ & + \cos^2(\phi/2) \sin^2(2\rho_{q-\beta}) \sin^2(a_{q-\beta}\tau) \\ & - \sin\phi \sin(2\rho_{q-\beta}) \sin(a_{q-\beta}\tau) [\cos(2\beta\theta - 4q\beta\tau) \cos(2\rho_{q+\beta}) \sin(a_{q+\beta}\tau) \\ & + \sin(2\beta\theta - 4q\beta\tau) \cos(a_{q+\beta}\tau)] \}, \end{aligned} \quad (18)$$

and

$$\begin{aligned} n_{\downarrow}(\theta, \tau) = & \frac{1}{2\pi} \{ \cos^2(\phi/2) [\cos^2(a_{q-\beta}\tau) + \cos^2(2\rho_{q-\beta}) \sin^2(a_{q-\beta}\tau)] \\ & + \sin^2(\phi/2) \sin^2(2\rho_{q+\beta}) \sin^2(a_{q+\beta}\tau) \\ & + \sin\phi \sin(2\rho_{q+\beta}) \sin(a_{q+\beta}\tau) [\cos(2\beta\theta - 4q\beta\tau) \cos(2\rho_{q-\beta}) \sin(a_{q-\beta}\tau) \\ & + \sin(2\beta\theta - 4q\beta\tau) \cos(a_{q-\beta}\tau)] \}. \end{aligned} \quad (19)$$

-
- | | |
|--|---|
| <p>[1] Aharonov Y and Bohm D 1959 <i>Phys. Rev.</i> 115 485.
 [2] Tsui D C, Stormer H L and Gossard A C 1982 <i>Phys. Rev. Lett.</i> 48 1559.
 [3] Laughlin R B 1983 <i>Phys. Rev. Lett.</i> 50 1395.
 [4] Stenger J, et al 1998 <i>Nature</i> 396 345.
 [5] Dalibard J, Gerbier F, Juzeliunas G, and Ohberg P 2011 <i>Rev. Mod. Phys.</i> 83 1523.
 [6] Zhai H 2012 <i>Int. J. Mod. Phys. B</i> 26 1230001.</p> | <p>[7] Galitski V and Spielman I B 2013 <i>Nature</i> 494 49.
 [8] Goldman N, Juzeliunas G, Ohberg P and Spielman I B 2014 <i>Rep. Prog. Phys.</i> 77 126401.
 [9] Zhai H 2014 arXiv:1403.8021v1 [cond-mat.quant-gas].
 [10] Osterloh K, Baig M, Santos L, Zoller P and Lewenstein M 2005 <i>Phys. Rev. Lett.</i> textbf95 010403.
 [11] Ruseckas J, Juzeliunas G, Ohberg P and Fleischhauer M 2005 <i>Phys. Rev. Lett.</i> 95 010404.</p> |
|--|---|

- [12] Zhu S L, Fu H, Wu C J, Zhang S C and Duan L M 2006 *Phys. Rev. Lett.* **97** 240401.
- [13] Liu X J, Borunda M F, Liu X and Sinova J 2009 *Phys. Rev. Lett.* **102** 046402.
- [14] Juzeliunas G, Ruseckas J and Dalibard J 2010 *Phys. Rev. A* **81** 053403.
- [15] Anderson B M, Juzeliunas G, Galitski V M and Spielman I B 2012 *Phys. Rev. Lett.* **108** 235301.
- [16] Lin Y J, Compton R L, Perry A R, Phillips W D, Porto J V and Spielman I B 2009 *Phys. Rev. Lett.* **102** 130401.
- [17] Lin Y J, Compton R L, Jiménez-García K, Porto J V and Spielman I B 2009 *Nature* **462** 628.
- [18] Lin Y J, Compton R L, Jiménez-García K, Phillips W D, Porto J V and Spielman I B 2011 *Nat. Phys.* **7** 531.
- [19] Lin Y J, Jiménez-García K and Spielman I B 2011 *Nature* **471** 83.
- [20] Beattie S, Moulder S, Fletcher R J and Hadzibabic Z 2013 *Phys. Rev. Lett.* **110** 025301.
- [21] Zhang J Y, et al 2012 *Phys. Rev. Lett.* **109** 115301.
- [22] Li Y, Martone G I, Stringari S 2012 *EPL* **99** 56008.
- [23] Ozawa t, Pitaevskii L P, Stringari S 2013 *Phys. Rev. A* **87** 063610.
- [24] Chen Z, Zhai H 2012 *Phys. Rev. A* **86** 041604(R).
- [25] Gupta S, Murch K W, Moore K L, Purdy T P and Stamper-Kurn D M 2005 *Phys. Rev. Lett.* **95** 143201.
- [26] Arnold A S, Garvie C S and Riis E 2006 *Phys. Rev. A* **73** 041606.
- [27] Ryu C, Andersen M F, Cladé P, Natarajan V, Helmerson K and Phillips W D 2007 *Phys. Rev. Lett.* **99** 260401.
- [28] Henderson K, Ryu C, MacCormick C and Boshier M G 2009 *New J. Phys.* **11** 043030.
- [29] Ramanathan A, Wright K C, Muniz S R, Zelan M, Hill W T, Lobb C J, Helmerson K, Phillips W D and Campbell G K 2011 *Phys. Rev. Lett.* **106** 130401.
- [30] Sherlock B E, Gildemeister M, Owen E, Nugent E and Foot C J 2011 *Phys. Rev. A* **83** 043408.
- [31] Moulder S, Beattie S, Smith R P, Tammuz N and Hadzibabic Z 2012 *Phys. Rev. A* **86** 013629.
- [32] Wright K C, Blakastal R B, Lobb C J, Phillips W P and Campbell G K 2012 arXiv:1208.3608.
- [33] Xue Rui, Li Wei-Dong, Liang Zhao-Xin 2014 *Chinese Physics Letters*, **31**, 030302.
- [34] Zheng W and Li Z B 2012 *Phys. Rev. A* **85** 053607.
- [35] Li Y, Martone G I, Pitaevskii L P and Stringari S 2013 *Phys. Rev. Lett.* **110** 235302.